


# Tuning Transduction from Hidden Observables to Optimize Information Harvesting

Giorgio Nicoletti<sup>1,\*</sup> and Daniel Maria Busiello<sup>2,†</sup>

<sup>1</sup>*ECHO Laboratory, École Polytechnique Fédérale de Lausanne, Lausanne, Switzerland*

<sup>2</sup>*Max Planck Institute for the Physics of Complex Systems, Dresden, Germany*

 (Received 14 March 2024; revised 20 June 2024; accepted 13 August 2024; published 7 October 2024)

Biological and living organisms sense and process information from their surroundings, typically having access only to a subset of external observables for a limited amount of time. In this Letter, we uncover how biological systems can exploit these accessible degrees of freedom to transduce information from the inaccessible ones with a limited energy budget. We find that optimal transduction strategies may boost information harvesting over the ideal case in which all degrees of freedom are known, even when only finite-time trajectories are observed, at the price of higher dissipation. We apply our results to red blood cells, inferring the implemented transduction strategy from membrane flickering data and shedding light on the connection between mechanical stress and transduction efficiency. Our framework offers novel insights into the adaptive strategies of biological systems under nonequilibrium conditions.

DOI: 10.1103/PhysRevLett.133.158401

Understanding how biological systems sense and process information from their surroundings is a long-standing question [1–4]. A fundamental problem is that these systems cannot typically access all the degrees of freedom (DOFs) characterizing the external world. Rather, they must rely on a subset of stochastic observables transmitting such external information to their internal processes. This transduction mechanism is made even more challenging by the intrinsic spatiotemporal limitations of the accessible trajectories, e.g., chemical concentrations [5–7] or positions in space [8–11]. How transduction allows for efficient information harvesting is far from being understood. Several works on signaling pathways highlighted that any information-processing operation inevitably requires energy [12–15], with theoretical limits on sensing of noisy variables [4–6,16]. However, very little is known about how much information on inaccessible observables is contained in the accessible ones. This is especially relevant since all biological systems operate with a limited energy budget. As a consequence, they have to tune their transduction strategies accordingly to achieve the maximal amount of information on the hidden DOFs. Moreover, the presence of multiple timescales [17–21], the

nonreciprocity of the interactions [22,23], and the intrinsic activity of biological systems [24] make the identification of optimal strategies a formidably complex task.

In this Letter, we tackle these problems and show that optimal transduction strategies may boost information harvesting over the ideal case in which all DOFs are known. We start by studying a hierarchical model, where a particle is coupled nonreciprocally to an intermediate observable that relays the information of a hidden DOF. The transduction strategy is implemented by tuning the coupling strength. We analytically identify the regimes in which the dissipation due to the unobservable DOF either prevents transduction or makes it inefficient over the ideal case, and show that efficient transduction inevitably causes an increase in both information variance and dissipation rate. However, biological systems usually extract information from stochastic trajectories on the fly. Hence, we study how the observation time of such trajectories affects the optimal transduction coupling. Finally, we extend our framework to analyze experimental data on red blood cells (RBCs). We quantify how much information on cytoskeleton activity is transduced into membrane flickering, unraveling the connection between transduction strategies and dissipation and highlighting intriguing differences in performance depending on mechanical conditions.

To fix the ideas, consider a membrane flickering due to the activity of an internal bath  $\eta$  (e.g., the cytoskeleton for RBCs [25]). The membrane undulations  $x$  are measured by an external biological or artificial probe  $y$  through a coupling parameter  $a$ . This coupling may be nonreciprocal, since the probe may not influence membrane motion. Thus, we have the following hierarchical active

\*Contact author: giorgio.nicoletti@epfl.ch

†Contact author: busiello@pks.mpg.de

*Published by the American Physical Society under the terms of the Creative Commons Attribution 4.0 International license. Further distribution of this work must maintain attribution to the author(s) and the published article's title, journal citation, and DOI. Open access publication funded by the Max Planck Society.*

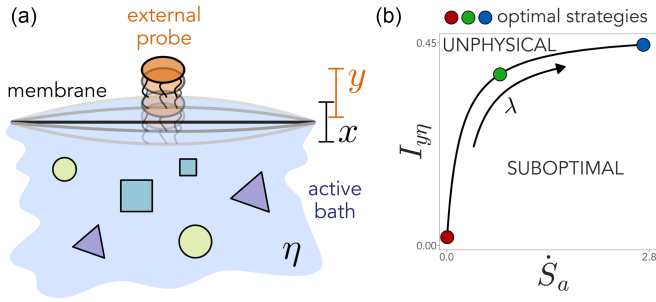


FIG. 1. (a) Sketch of the model. Membrane fluctuations  $x$  transduce information from an active bath  $\eta$  to a probe  $y$ . (b) Pareto front. Mutual information between  $y$  and  $\eta$  is maximized while minimizing dissipation. Transduction strategies correspond to different points on the optimal front.  $\theta_\eta = 5$ ,  $\sigma = 1$ .

model [Fig. 1(a)]:

$$\begin{aligned}\tau_y \dot{y} &= -y + ax + \sqrt{2\tau_y D_y} \xi_y(t), \\ \tau_x \dot{x} &= -x + \sigma\eta + \sqrt{2\tau_x D_x} \xi_x(t), \\ \tau_\eta \dot{\eta} &= -\eta + \sqrt{2\tau_\eta D_\eta} \xi_\eta(t),\end{aligned}\quad (1)$$

where  $\sigma$  is the bath-membrane coupling,  $\xi_i$  white noises,  $D_i$  diffusion coefficients, and  $\tau_i$  the typical timescales, with  $i = x, y, \eta$ . Since the probe has to harvest information on  $\eta$  without being able to interact with it directly, we focus on the role of the indirect coupling  $a$ , which the probe must tune to optimize the transduction of information from the bath. We fix  $D_x = D_y = D_\eta = 1$  and  $\tau_x = \tau_y = \tau = 1$ . A leading role is played by both  $\sigma$ , which controls the membrane-bath dissipation, and  $\tau_\eta \equiv \tau\theta_\eta$ , dictating whether the activity is averaged out or not [17].

The task of the probe is to extract information on the bath. Consider first the ideal case in which all DOFs are accessible, so that the probe can directly maximize the mutual information between  $\eta$  and itself  $I_{y\eta}$  and minimize the dissipation induced by its coupling to the membrane,  $\dot{S}_a = \dot{S}_{\text{tot}} - \dot{S}_{\text{tot}}|_{a=0}$ . This amounts to finding the coupling  $a^*$  that maximizes the Pareto functional  $\mathcal{L}(a)$  [26,27]:

$$a^* = \arg \max_a \underbrace{(\lambda I_{y\eta} - (1 - \lambda)T\dot{S}_a)}_{\mathcal{L}(a)}, \quad (2)$$

where  $T$  is taken as unit time and  $0 < \lambda < 1$ . Since information and dissipation are usually in trade-off [14], an optimal front characterizing transduction in different regimes naturally emerges [Fig. 1(b)]. We remark that the functional approach proposed here should be seen as an *a posteriori* description of the system, rather than an *a priori* design principle [2,4,28,29].

The parameter  $\lambda$  represents the strategy that the probe implements. For small  $\lambda$ , the probe is acting to

preferentially minimize dissipation, while a high  $\lambda$  denotes an information-driven strategy. Thus,  $\lambda$  indirectly sets the system's energy budget (see Supplemental Material [30]). At stationarity, we evaluate analytically the mutual information between  $y$  and  $\eta$ :

$$I_{y\eta} = \frac{1}{2} \log \frac{(\mathbf{\Sigma})_{yy} (\mathbf{\Sigma})_{\eta\eta}}{\det(\mathbf{\Sigma}_{y\eta})}, \quad (3)$$

where  $(\mathbf{\Sigma})_{ij}$  are the entries of the covariance matrix of the system  $\mathbf{\Sigma}$ , and  $\mathbf{\Sigma}_{ij}$  is the corresponding submatrix on variables  $i$  and  $j$ . Similarly, the dissipation is

$$\dot{S}_{\text{tot}} = \text{Tr}(\mathbf{D}^{-1} \mathbf{A} \mathbf{\Sigma} \mathbf{A}^T) - \text{Tr}(\mathbf{A}), \quad (4)$$

with  $\mathbf{A}$  and  $\mathbf{D}$  the interaction and diffusion matrices associated with Eq. (1) (see Ref. [30] for explicit derivations).

However, this ideal scenario cannot be realized. Being only coupled to  $x$ , the probe does not have access to the evolution of  $\eta$ . Thus, both  $I_{y\eta}$  and  $\dot{S}_a$  cannot be estimated directly, nor the functional in Eq. (2). From the stochastic trajectories seen by the probe, the only measurable quantities are instead its information with the membrane  $I_{xy}$  and the dissipation stemming from the observable DOFs  $\dot{S}_{xy}$ . Therefore, the probe must optimize an effective functional  $\mathcal{L}_{\text{eff}}$  to determine its effective transduction coupling:

$$a_{\text{eff}}^* = \arg \max_a \underbrace{(\lambda I_{xy} - (1 - \lambda)T\dot{S}_{xy})}_{\mathcal{L}_{\text{eff}}(a)}, \quad (5)$$

which, in general, is different from  $a^*$  [Figs. 2(a) and 2(b)].  $I_{xy}$  and  $\dot{S}_{xy}$  can be estimated as before, where  $\mathbf{\Sigma}$  and  $\mathbf{D}$  have to be substituted by the submatrices  $\mathbf{\Sigma}_{xy}$  and  $\mathbf{D}_{xy}$ , and  $\mathbf{A}$  by the reduced interaction matrix,

$$\mathbf{A}_{xy}^{\text{red}} = \mathbf{A}_{xy} + \mathbf{C} \mathbf{\Sigma}_{xy}^{-1}, \quad (\mathbf{C})_{ij} = (\mathbf{A})_{i\eta} (\mathbf{\Sigma})_{j\eta}, \quad (6)$$

with  $i, j = x, y$ .  $\mathbf{A}_{xy}^{\text{red}}$  is the interaction matrix appearing in the Fokker-Planck equation marginalized over  $\eta$  [30].

To evaluate the performance of transduction, we compare the mutual information between the probe and the bath in the ideal but unrealizable case  $I_{y\eta}(a^*)$  with the same quantity when the coupling takes its effective value  $I_{y\eta}(a_{\text{eff}}^*)$  [Fig. 2(c)]. We name  $I_{y\eta}(a^*)$  target information, while  $I_{y\eta}(a_{\text{eff}}^*)$  is the transduced information that the probe can effectively harvest. We analytically find that there exists a range of  $\sigma$  for which the transduced information is larger than the target information [Fig. 2(d)]. Since  $a_{\text{eff}}^*$  has been set by optimizing the accessible quantities in  $\mathcal{L}_{\text{eff}}$ , this unexpected result shows that transduction mechanisms may boost information over the ideal scenario. However, increasing  $\sigma$ , the membrane dynamics becomes dominated by the bath, inducing, in principle, a larger probe-membrane dissipation that cannot be counterbalanced

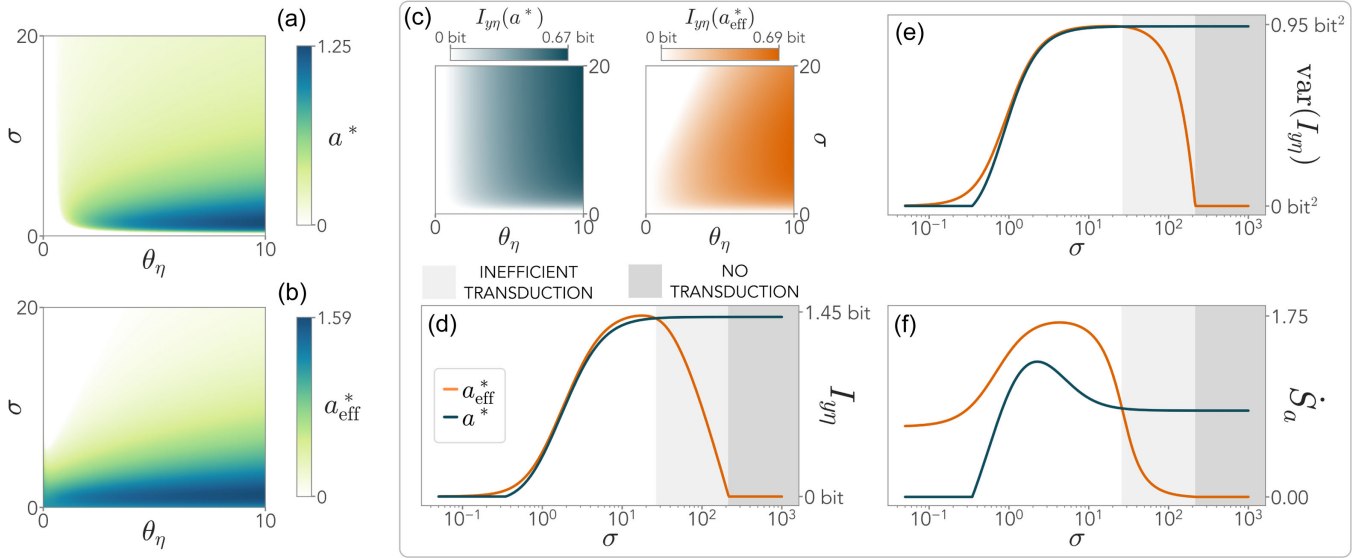


FIG. 2. (a),(b) Optimal coupling in the ideal case ( $a^*$ ) and considering only the accessible DOFs ( $a_{\text{eff}}^*$ ) as a function of membrane-bath interaction  $\sigma$  and activity timescale  $\theta_\eta$ . (c) Target information  $I_{y\eta}(a^*)$  (blue) and transduced information  $I_{y\eta}(a_{\text{eff}}^*)$  (orange). (d)–(f) Optimal transduction can boost information harvesting over the ideal case (d), at the expense of precision (e) and dissipation (f). Regimes of inefficient transduction appear at increasing  $\sigma$ . At a critical membrane-bath coupling, transduction is ineffective; thus no information can be harvested and dissipation comes only from the active bath.  $\lambda = 0.9$ , and  $\theta_\eta = 50$  for panels (d)–(f).

by  $I_{xy}$ . As a consequence,  $a_{\text{eff}}^*$  decreases to minimize  $\dot{S}_{xy}$ , and transduction first becomes inefficient and then disappears [Fig. 2(d)].

Yet, information transduction happens at a cost. Efficient transduction allows for more information to be harvested, but remains a suboptimal solution in terms of the full-knowledge functional due to the system being unable to correctly estimate the balance between information and dissipation [30]. Furthermore, the variance of  $I_{y\eta}$ , computed as

$$\text{var}(I_{y\eta}) = \frac{(\Sigma_{y\eta})^2}{(\Sigma)_{yy}(\Sigma)_{\eta\eta}}, \quad (7)$$

is also higher for efficient transduction, evidencing a reduction in processing precision [see Fig. 2(e) and [30]]. Analogously, the system exhibits higher dissipation in the same region of parameters, since harvesting more information requires more energy than in the ideal case [Fig. 2(f)]. Overall, once the probe fixes the balance between dissipation and information by choosing a strategy  $\lambda$ , the possibility of tuning the energy consumption is crucial for the onset of efficient transduction. Different choices of  $\lambda$  will change the value of  $\sigma$  at which transduction becomes inefficient, without qualitatively affecting the results. At small values of  $\theta_\eta$ , the active bath becomes a fast variable, and thus its mutual information with both  $x$  and  $y$  becomes negligible [9,17]. As a consequence,  $a^*$  is tuned to mainly minimize  $\dot{S}_a$ , leading to vanishingly small

target information and dissipation in the ideal case. In [30], we show that the crossovers between the different transduction regimes are influenced by the timescales  $\tau_x$  and  $\tau_y$ , which control how information propagates in the system [17]. In particular, the emergence of efficient transduction is related to how  $x$  shares information with  $y$ , and such information tends to increase when  $\tau_y \lesssim \tau_x$ .

Another pivotal complication that constrains the operations of biological systems is that they usually must tune their parameters from stochastic trajectories observed on the fly. In realistic scenarios, mutual information must instead be computed from stochastic trajectories as

$$i_{xy}(t) = \log \frac{p_{xy}(x(t), y(t))}{p_x(x(t))p_y(y(t))} \quad (8)$$

where  $p_{xy}(x(t), y(t))$ ,  $p_x(x(t))$ , and  $p_y(y(t))$  are the joint and marginalized distributions of  $x$  and  $y$  evaluated on each point of the trajectory  $\{x(t), y(t)\}$ . Clearly,  $I_{xy} = \langle i_{xy} \rangle$  and  $\text{var}(I_{xy}) = \langle i_{xy}^2 \rangle - \langle i_{xy} \rangle^2$ , where the average is performed over stationary trajectories [31–33]. Furthermore, we assume that the probabilities in Eq. (8) are the empirical probabilities estimated directly from trajectories. Then, the probe can estimate dissipation along a single trajectory as

$$\dot{s}_{xy}(t) = \mathbf{A}_{xy}^{\text{red}} \circ (\dot{x}(t), \dot{y}(t))^T, \quad (9)$$

where  $\circ$  indicates the Stratonovich product [34], and  $\dot{S}_{xy} = \langle \dot{s}_{xy} \rangle$  by plugging into the reduced interaction matrix

between  $x$  and  $y$ , Eq. (9) [35]. Therefore, we can define an effective functional that depends on the observation time  $T_A$ :

$$\mathcal{L}_{\text{tr}}(a, T_A) = \lambda \langle i_{xy} \rangle_{T_A} + (1 - \lambda) \langle \dot{s}_{xy} \rangle_{T_A}, \quad (10)$$

where averages are performed over trajectories of duration  $T_A$ . We name  $a_{\text{tr}}$  the coupling that maximizes  $\mathcal{L}_{\text{tr}}$ .

Consider now a biological probe that continuously adapts the probe-membrane coupling  $a_{\text{tr}}(N)$ , where  $N$  indicates the number of adaptive steps it has undergone. The probe stochastically selects a new coupling  $a_{\text{tr}}(N) + \Delta a$ , with  $\Delta a \sim \mathcal{N}(0, \sigma_a)$ . During a time  $T_A$ , it measures information and dissipation via Eqs. (8) and (9), resulting in an estimate of  $\mathcal{L}_{\text{tr}}(a, T_A)$ . Based on these temporally limited observations, the adaptive probe tests the performance of its coupling: if the estimated  $\mathcal{L}_{\text{tr}}(a, T_A)$  is larger than the previous one, it retains the proposed coupling, i.e.,  $a_{\text{tr}}(N+1) = a_{\text{tr}}(N) + \Delta a$ ; otherwise it discards it, and  $a_{\text{tr}}(N+1) = a_{\text{tr}}(N)$ . The dynamics proceeds until no new adaptive move is accepted for a sufficiently long stopping time; we assume that the system begins with no probe-membrane coupling. This adaptive dynamics (see Ref. [30] for details) leads the system to converge to a coupling that approaches the maximum of  $\mathcal{L}_{\text{eff}}$  for large measurement times  $T_A$  [Figs. 3(a) and 3(b)]. As  $T_A$  increases, both the number of adaptive steps until convergence and the variance among different realizations

decrease, whereas at small  $T_A$  the uncertainty on the empirical probability estimation leads to spurious values of  $I_{xy}$  [insets of Fig. 3(a)]. Indeed, the precision of information transduction,

$$\mathcal{P}(N) = \frac{\langle i_{y\eta} \rangle_{T_A}^2}{\langle i_{y\eta}^2 \rangle_{T_A} - \langle i_{y\eta} \rangle_{T_A}^2}, \quad (11)$$

increases with  $T_A$  [Fig. 3(c)]. In [30], we show that the results remain qualitatively similar if the true probability distribution is used instead of the empirical one.

Finally, we employ our framework to study transduction in red blood cells. Membrane flickering of RBCs is a well-known phenomenon [37] that takes place out of equilibrium in healthy cells and, as such, dissipates energy [25]. Flickering might tune cell-cell interactions [8], promote protein mobility on the membrane [38,39], and facilitate protein uptake [40]. All these processes are instrumental in establishing robust cellular functions, and their mechanisms are encoded in the motion of the outer membrane. Therefore, a pivotal question is understanding when and how membrane flickering carries information on the internal active cytoskeleton [41], transduced through the membrane layers of the lipid bilayer. Thus, even if our framework does not include details on the biochemical structure of RBCs, it may represent an effective tool to shed light on how the cells dissipate energy to transduce information. To this end, we consider a recent model that was shown to quantitatively capture dynamic and thermodynamic properties of RBCs flickering [42], and that is remarkably similar to Eq. (1), with the addition of a reciprocal interaction  $k_{\text{int}}$  between the inner and outer membrane layer [Fig. 4(a)] [30]. We include the mobility of both membrane layers,  $\mu_x$  and  $\mu_y$ , and we enforce the fluctuation-dissipation relation to fix the diffusion coefficients,  $D_x = \beta^{-1} \mu_x$  and  $D_y = \beta^{-1} \mu_y$ , with  $\beta = (k_B T)^{-1}$ ,  $k_B$  the Boltzmann constant and  $T$  the temperature. The cytoskeleton now plays the role of the hidden DOF  $\eta$ . The inner membrane is the transducing degree of freedom  $x$ , while  $y$  is the outer membrane. Experimental data from optical sensing, microscopy, and trapping allowed for direct measurement of all model parameters in [42]. Using such estimations, we find a net distinction between passive and healthy (active) RBCs. Crucially, active RBCs exhibit substantially higher values of heat dissipation and the mutual information  $I_{y\eta}$  between the outer membrane and the cytoskeleton, indicating that information is being transduced through the lipid bilayer [red points in Fig. 4(a)].

The estimated energy dissipation of each RBC stems from the coupling between the cytoskeleton and inner membrane only. Therefore, we can infer the value of  $\lambda$  that allows information transduction from the cytoskeleton to flickering and is compatible with the measured energy budget. In practice, we determine  $\lambda$  for each RBC such that the experimental  $k_{\text{int}}$  corresponds to the maximum of  $\mathcal{L}_{\text{eff}}$ .

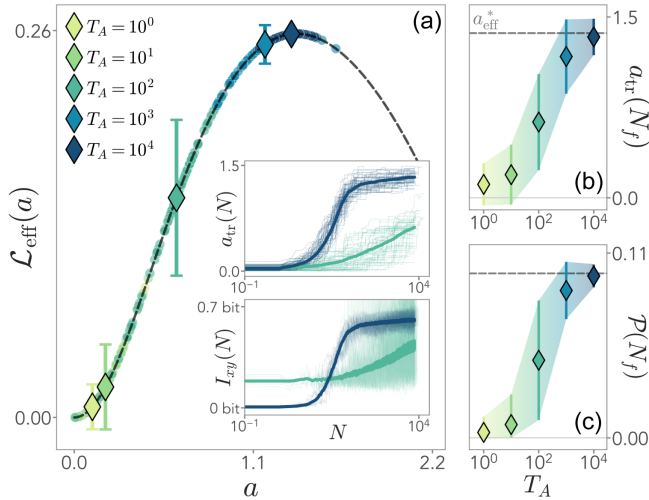


FIG. 3. (a) Increasing the observation time  $T_A$ , the probe adaptive dynamics approaches the maximum of  $\mathcal{L}_{\text{tr}}$ . Diamonds represent average values of the functional, and insets show the optimal coupling and estimated information for two values of  $T_A$  ( $10^2$  and  $10^4$ ) versus the number of adaptive steps  $N$  for 320 realizations. At small  $T_A$ , uncertainties in the empirical distribution estimation lead to nonzero  $I_{xy}$  even for  $a \approx 0$ . (b),(c) Optimal coupling (b) and information precision (c) estimated from stochastic trajectories at the final step  $N = N_f$  for increasing  $T_A$ . The shaded area indicates one standard deviation.



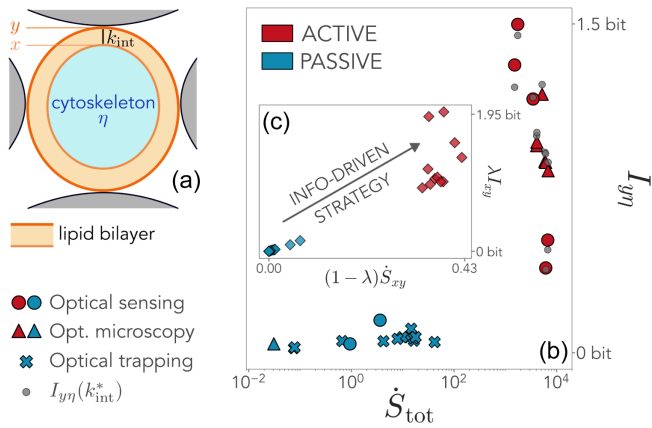


FIG. 4. (a) Sketch of the model for RBCs. Cytoskeleton activity  $\eta$  is transduced into the flickering of the outer membrane  $y$  through the inner membrane  $x$  of the lipid bilayer. (b) Information-dissipation balance for passive and active RBCs in different experiments. (c) Increasing dissipation, information becomes more important for the transduction strategies.

We find that the strategy becomes more information driven, i.e.,  $\lambda I_{xy} \gg (1-\lambda)\dot{S}_{xy}$ , for more active RBCs [Fig. 4(c)]. This shows that the internal parameters are tuned so that the higher the available energy, the greater the information that membrane flickering harvests from the active cytoskeleton. We also uncover an intriguing relationship between mechanical stress and transduction efficiency. First, we compute the target information,  $I_{y\eta}(k_{int}^*)$ , at the same value of  $\lambda$  [gray dots in Fig. 4(b)], where  $k_{int}^*$  is the optimal coupling that the RBC would choose if the outer membrane had direct access to the state of the cytoskeleton, maximizing Eq. (2). This comparison is analogous to the one shown in Fig. 2(d). Among active RBCs, we find that transduction is inefficient in experiments performed with optical microscopy, while optical sensing is associated with an efficient regime [Fig. 4(b)]. Indeed, in these two settings, cells are held in their position with different setups (details about the experiments are found in [42]) and exhibit different mechanical properties known to crucially affect their functional behavior [43–45]. This naturally translates into the change in the transduction performance highlighted by our framework, suggesting a promising path for functional investigations of biological systems in different conditions.

In this Letter, we uncovered how biological systems can harvest information on hidden DOFs by tuning their couplings to accessible observables. We found that, in certain regimes, transduced information can overcome the ideal case in which all the DOFs are known, even when only finite-time stochastic trajectories can be measured. These results hint at the existence of intrinsic and crucial constraints on internal parameters of biological systems that allow for efficient transduction mechanisms. We applied our framework to evaluate, for the first time,

how membrane flickering in RBCs transduces information from the cytoskeleton to the outer membrane, revealing an intriguing link between mechanical stress and transduction performances. In [30], we discuss possible ways to substantiate our choice for the optimization functional, such as the evaluation of transduction efficiency along RBC membrane and multivariate dynamical recordings. We also show that eliminating an explicit constraint on the energy budget leads to a diverging dissipation to maintain transduction efficiency. Finally, extending our framework to path mutual information between trajectories [46,47] will allow us to study nonstationary conditions during real-time information processing.

Our Letter can be extended to different biological organisms, allowing for a deeper characterization of the relationship between systems’ activity and functional behaviors. Indeed, although dissipation is usually associated with healthy conditions, it is not necessarily tangled with robust cellular function, such as efficient information transduction. Ultimately, our results shed light on how nonequilibrium conditions and information harvesting shape biological systems.

*Acknowledgments*—G. N. acknowledges funding provided by the Swiss National Science Foundation through its Grant No. CRSII5\_186422. The authors thank Matteo Ciarchi and Marco Baiesi for useful comments and suggestions, and Ivan Di Terlizzi for insightful discussions on the RBC model. They also thank the Max Planck Institute for the Physics of Complex Systems for hosting G. N. during the final phase of this work.

- [1] W. Bialek and S. Setayeshgar, Physical limits to biochemical signaling, *Proc. Natl. Acad. Sci. U.S.A.* **102**, 10040 (2005).
- [2] G. Tkačik and W. Bialek, Information processing in living systems, *Annu. Rev. Condens. Matter Phys.* **7**, 89 (2016).
- [3] E. Kussell and S. Leibler, Phenotypic diversity, population growth, and information in fluctuating environments, *Science* **309**, 2075 (2005).
- [4] M. Bauer and W. Bialek, Information bottleneck in molecular sensing, *PRX Life* **1**, 023005 (2023).
- [5] K. Kaizu, W. De Ronde, J. Pajmans, K. Takahashi, F. Tostevin, and P.R. Ten Wolde, The Berg-Purcell limit revisited, *Biophys. J.* **106**, 976 (2014).
- [6] T. Mora and I. Nemenman, Physical limit to concentration sensing in a changing environment, *Phys. Rev. Lett.* **123**, 198101 (2019).
- [7] H. C. Berg and E. M. Purcell, Physics of chemoreception, *Biophys. J.* **20**, 193 (1977).
- [8] E. Evans and V. Parsegian, Thermal-mechanical fluctuations enhance repulsion between bimolecular layers, *Proc. Natl. Acad. Sci. U.S.A.* **83**, 7132 (1986).
- [9] G. Nicoletti and D.M. Busiello, Mutual information disentangles interactions from changing environments, *Phys. Rev. Lett.* **127**, 228301 (2021).

- [10] G. Nicoletti and D. M. Busiello, Mutual information in changing environments: Nonlinear interactions, out-of-equilibrium systems, and continuously varying diffusivities, *Phys. Rev. E* **106**, 014153 (2022).
- [11] G. Nicoletti, A. Maritan, and D. M. Busiello, Information-driven transitions in projections of underdamped dynamics, *Phys. Rev. E* **106**, 014118 (2022).
- [12] R. Cheong, A. Rhee, C. J. Wang, I. Nemenman, and A. Levchenko, Information transduction capacity of noisy biochemical signaling networks, *Science* **334**, 354 (2011).
- [13] T. Sagawa and M. Ueda, Minimal energy cost for thermodynamic information processing: Measurement and information erasure, *Phys. Rev. Lett.* **102**, 250602 (2009).
- [14] G. Lan, P. Sartori, S. Neumann, V. Sourjik, and Y. Tu, The energy–speed–accuracy trade-off in sensory adaptation, *Nat. Phys.* **8**, 422 (2012).
- [15] C. C. Govern and P. R. ten Wolde, Energy dissipation and noise correlations in biochemical sensing, *Phys. Rev. Lett.* **113**, 258102 (2014).
- [16] G. Malaguti and P. R. Ten Wolde, Theory for the optimal detection of time-varying signals in cellular sensing systems, *eLife* **10**, e62574 (2021).
- [17] G. Nicoletti and D. M. Busiello, Information propagation in multilayer systems with higher-order interactions across timescales, *Phys. Rev. X* **14**, 021007 (2024).
- [18] G. Nicoletti, M. Bruzzone, S. Suweis, M. Dal Maschio, and D. M. Busiello, Information gain at the onset of habituation to repeated stimuli, [arXiv:2301.12812](https://arxiv.org/abs/2301.12812).
- [19] S. Bo and A. Celani, Multiple-scale stochastic processes: Decimation, averaging and beyond, *Phys. Rep.* **670**, 1 (2017).
- [20] B. Mariani, G. Nicoletti, M. Bisio, M. Maschietto, S. Vassanelli, and S. Suweis, Disentangling the critical signatures of neural activity, *Sci. Rep.* **12**, 10770 (2022).
- [21] D. M. Busiello, D. Gupta, and A. Maritan, Coarse-grained entropy production with multiple reservoirs: Unraveling the role of time scales and detailed balance in biology-inspired systems, *Phys. Rev. Res.* **2**, 043257 (2020).
- [22] S. H. Klapp, Non-reciprocal interaction for living matter, *Nat. Nanotechnol.* **18**, 8 (2023).
- [23] D. M. Busiello, M. Ciarchi, and I. Di Terlizzi, Unraveling active baths through their hidden degrees of freedom, *Phys. Rev. Res.* **6**, 013190 (2024).
- [24] X. Fang, K. Kruse, T. Lu, and J. Wang, Nonequilibrium physics in biology, *Rev. Mod. Phys.* **91**, 045004 (2019).
- [25] H. Turlier, D. A. Fedosov, B. Audoly, T. Auth, N. S. Gov, C. Sykes, J.-F. Joanny, G. Gompper, and T. Betz, Equilibrium physics breakdown reveals the active nature of red blood cell flickering, *Nat. Phys.* **12**, 513 (2016).
- [26] L. F. Seoane and R. Solé, Phase transitions in Pareto optimal complex networks, *Phys. Rev. E* **92**, 032807 (2015).
- [27] L. Koçillari, P. Fariselli, A. Trovato, F. Seno, and A. Maritan, Signature of Pareto optimization in the *Escherichia coli* proteome, *Sci. Rep.* **8**, 9141 (2018).
- [28] N. Tishby, F. C. Pereira, and W. Bialek, The information bottleneck method, [arXiv:physics/0004057](https://arxiv.org/abs/physics/0004057).
- [29] E. Schneidman, M. J. Berry, R. Segev, and W. Bialek, Weak pairwise correlations imply strongly correlated network states in a neural population, *Nature (London)* **440**, 1007 (2006).
- [30] See Supplemental Material at <http://link.aps.org/supplemental/10.1103/PhysRevLett.133.158401> for mathematical details, analytical derivations, and model details.
- [31] J. M. Parrondo, J. M. Horowitz, and T. Sagawa, Thermodynamics of information, *Nat. Phys.* **11**, 131 (2015).
- [32] L. Dabelow, S. Bo, and R. Eichhorn, Irreversibility in active matter systems: Fluctuation theorem and mutual information, *Phys. Rev. X* **9**, 021009 (2019).
- [33] S. Pigolotti, I. Neri, É. Roldán, and F. Jülicher, Generic properties of stochastic entropy production, *Phys. Rev. Lett.* **119**, 140604 (2017).
- [34] C. W. Gardiner, *Handbook of Stochastic Methods for Physics, Chemistry and the Natural Sciences*, 3rd ed., Springer Series in Synergetics (Springer-Verlag, Berlin, 2004).
- [35] Here, we are ignoring the errors induced by force field inference from finite-time trajectories [36]. For simplicity, we consider instead the analytical interaction matrix, which assumes that the system can correctly estimate it for any trajectory duration.
- [36] A. Frishman and P. Ronceray, Learning force fields from stochastic trajectories, *Phys. Rev. X* **10**, 021009 (2020).
- [37] T. Browicz, Further observation of motion phenomena on red blood cells in pathological states, *Zbl. Med. Wiss.* **28**, 625 (1890).
- [38] F. L. Brown, Regulation of protein mobility via thermal membrane undulations, *Biophys. J.* **84**, 842 (2003).
- [39] L. C.-L. Lin and F. L. Brown, Dynamics of pinned membranes with application to protein diffusion on the surface of red blood cells, *Biophys. J.* **86**, 764 (2004).
- [40] Y. A. Ayala, R. Omidvar, W. Römer, and A. Rohrbach, Thermal fluctuations of the lipid membrane determine particle uptake into giant unilamellar vesicles, *Nat. Commun.* **14**, 65 (2023).
- [41] R. Rodríguez-García, I. López-Montero, M. Mell, G. Egea, N. S. Gov, and F. Monroy, Direct cytoskeleton forces cause membrane softening in red blood cells, *Biophys. J.* **108**, 2794 (2015).
- [42] I. D. Terlizzi, M. Gironella, D. Herraez-Aguilar, T. Betz, F. Monroy, M. Baiesi, and F. Ritort, Variance sum rule for entropy production, *Science* **383**, 971 (2024).
- [43] M. Dao, C. T. Lim, and S. Suresh, Mechanics of the human red blood cell deformed by optical tweezers, *J. Mech. Phys. Solids* **51**, 2259 (2003).
- [44] S. Suresh, Mechanical response of human red blood cells in health and disease: Some structure-property-function relationships, *J. Mater. Res.* **21**, 1871 (2006).
- [45] G. Tomaiuolo, Biomechanical properties of red blood cells in health and disease towards microfluidics, *Biomicrofluidics* **8**, 051501 (2014).
- [46] F. Tostevin and P. Rein ten Wolde, Mutual information between input and output trajectories of biochemical networks, *Phys. Rev. Lett.* **102**, 218101 (2009).
- [47] M. Reinhardt, G. Tkačik, and P. R. ten Wolde, Path weight sampling: Exact Monte Carlo computation of the mutual information between stochastic trajectories, *Phys. Rev. X* **13**, 041017 (2023).